VOLUME 17 January 2020 eISSN : 2382-5340 ISSN : 2091 - 0762

Journal of Physical Sciences

BIBECHANA

Editor-in-Chief

Devendra Adhikari

Professor, Physics

MMAMC, T.U.

Published by

Department of Physics

Mahendra Morang Adrash Multiple Campus

T.U., Biratnagar

www.nepjol.info/index.php/BIBECHANA

BIBECHANA
ISSN 2091-0762 (Print), 2382-5340 (Online)
Journal homepage: http://nepjol.info/index.php/BIBECHANA
Publisher: Department of Physics, Mahendra Morang A.M. Campus, TU, Biratnagar, Nepal

Comparative studies on the electronic transport in magnetically quantized low band gap semiconductor system

S. Shrestha[1*], C. K. Sarkar[2]
[1]Central Department of Physics, Tribhuvan University, Kathmandu, Nepal
[2]Department of ETCE, Jadavpur University, Kolkata, India
[*]Email: sanju12np@yahoo.com

Article Information
Received: November 19, 2018
Accepted: September 28, 2019

Keywords:
High magnetic field
Figure of Merit
Mercury Cadmium Telluride
Electron transport

ABSTRACT

The Q1D system formed by magnetically confined system is attracting attention of researchers in device application because it is capable of over-looking the various techniques of fabrication difficulties and defects created by such fabrication techniques. In the presence of a high magnetic field, the transverse component of the energy dispersion relation gets quantized into various equally spaced energy levels called Landau levels and the motion of the carriers is completely restricted. However, the longitudinal component along the field is still free to move. The mobility of such system is enhanced when a low effective mass semiconductors n-HgCdTe (Mercury Cadmium Telluride) is used. The band structure of n-HgCdTe is found to be nonparabolic due to its low band gap according to Kane [Phadke and Sharma, 1975]. Recent publications, based on experimental verifications of transport coefficient of n-HgCdTe of Chen and Sher [Chen and Sher, 1982] show that the band structure of Mercury Cadmium Telluride (MCT) is more hyperbolic in nature rather than nonparabolic. The author has compared the effect of band structures on the various transport properties of MCT such as mobility, Seebeck coefficient, thermal conductivity, figure of merit (Z) etc. The figure of merit is a very important property of a material to be used in thermoelectric devices, such as cooler, refrigerator etc. The product of Z and temperature i.e. (ZT), a dimensionless quantity is found to be maximum for parabolic band structure and is followed by nonparabolic and hyperbolic band structures for all ranges of variation of temperature as well as magnetic field. Taking the hyperbolic band structure of MCT, the effect of high and low temperature scattering mechanisms on ZT is also observed.

DOI: https://doi.org/10.3126/bibechana.v17i0.21741

1. Introduction

The quasi-one dimensional (Q1D) system formed by magnetically confined system is attracting attention of researchers in device application because it is capable of over-looking the various techniques of fabrication difficulties and defects created by such fabrication techniques.

In the presence of high magnetic field, the electrons in sample move into a helical path due to the Lorentz force in the direction transverse to the

magnetic field. The energy of such electrons are quantized into various energy levels called the Landau levels [1]. However, the motion of the electrons in the longitudinal direction i.e. along the direction of the magnetic field is still free to move, such a system behaves as a quasi-one dimensional (Q1D) system. At a reasonable high magnetic field, electrons would occupy only the lowest Landau level and the condition is called the extreme quantum limit (EQL). To simplify our calculations we have considered the case EQL in our work.

The thermal transport property of semiconductors characterized by figure of merit of thermoelectric is defined as $Z = S^2\sigma/\kappa$ [2-4], where σ, S and κ are the electrical conductivity, Seebeck coefficient and the thermal conductivity respectively. Z has the dimension of inverse temperature. If we are trying to pump heat from cooler region to hotter one, we need high pumping efficiency (high S), low backward conduction of heat (low κ) and low production of heat through Joule heating (high σ) [5]. High mobility is inherently important to facilitate electron transport in the thermoelectric materials to reduce the Joule heating [6].

$Hg_{0.8}Cd_{0.2}Te$ (MCT) is a narrow-direct band gap and alloy semiconductor useful for various electronics and optoelectronic devices for different applications such as infrared detectors [6], thermoelectric devices such as cooler (7), refrigerator etc. Due to the narrow band gap, MCT has very low effective mass. Hence MCT has a very high conductivity, is necessary to optimize the performance of thermoelectric devices. Also, due to the narrow band gap, the band structure of MCT is highly nonparabolic and the nonparabolicity has been calculated based on Kane's model [8]. The study of Chen and Sher [9], shows that the band structure of MCT is more hyperbolic in nature rather than nonparabolic, as described by Kane in order to explain the transport parameters of MCT.

In the present paper, we have calculated the thermoelectric figure of merit (Z) of magnetically confined Q1D system of MCT. The effect of the band structures on Z is also studied.

The effect of various low temperature scattering mechanisms such as ionized impurity (in), alloy disorder (all), acoustic phonon via deformation potential (ac) and piezoelectric (pz) scattering mechanisms and high temperature scattering mechanism such as polar optical phonon (pop) scattering mechanism [8,10,11] on the figure of merit Z is also examined assuming nondegenerate carrier distributions for electrons.

2. Theoretical Formulation

Band structures of MCT

We consider a semiconductor with nonparabolic spherically symmetric conduction band subjected to a large longitudinal quantizing magnetic field B along z-axis which causes the electrons to occupy the lowest Landau level i.e. Extreme Quantum Limit (EQL). A temperature gradient ΔT is also applied along the z-axis. The Boltzmann transport equation can be used for the longitudinal configuration since the magnetic quantization does not produce any effect on the longitudinal motion of charge carriers. The energy dispersion relation for electrons is given below for nonparabolic band based on Kane's model [8],

$$E^{np} = \frac{\hbar^2 k_z^2}{2m^* a_o} + \left(n + \frac{1}{2}\right) E_g (a_o - 1) \quad \ldots (1)$$

where, the 1st term in the equation (1), $\hbar^2 k_z^2 / 2m^* a_0$ gives the longitudinal component of energy (E_{oz}) along z-axis. In the expression k_z be the z-component of the wave vector. m^* and $\hbar$ are the effective mass and Planck's constant divided by 2π respectively. The second term of the equation (1), gives transverse component of quantized energy along xy-plane due to the presence of magnetic field, where, E_g is the band gap energy. n is Landau subband index and a_o being the nonparabolicity factor is given as,

$$a_o = \left[1 + 2\hbar\omega_c \left(1 - |g|\frac{m^*}{2m_o}\right) \Big/ E_g\right]^{1/2} \quad \ldots (2)$$

In the equation (2), $|g|$ and $\omega_c = (Be/m^*)$ be the Lande's g-factor and the cyclotron frequency respectively; Where e, m_o and B are the charge of an electron, free electron mass and magnetic flux density respectively.

The wide band gap parabolic semiconductor material means E_g to be large i.e. $E_g \to \infty$. In such condition $a_o \to 1$. Hence, nonparabolicity factor (a_o) reduces to unity. The energy dispersion relation given by equation (1) for nonparabolic band structure reduces to parabolic relation and is given as below,

$$E^p = \frac{\hbar^2 k_z^2}{2m*} + \left(n + \frac{1}{2}\right)\hbar\omega_c\left(1 - |g|\frac{m^*}{m_o}\right)... \quad (3)$$

For the sake of interpretation of the experimental transport results, Krishnamurthy and Sher [12] suggested the hyperbolic band relation for narrow band gap semiconductors such as MCT, and is given in the following form,

$$E^h = \left(\gamma k^2 + c^2\right)^{\frac{1}{2}} - c... \quad (4)$$

where,

$$k^2 = \left(n + \frac{1}{2}\right)\frac{2eB}{\hbar} + k_z^2... \quad (5)$$

The terms γ and c in equation (4) are adjustable parameters to fit the experimental data[13]. The hyperbolic band structure of equation (4) is simplified in a form to make a comparative study with parabolic and nonparabolic band structures. The hyperbolic band relation given by equation (4) reduces to the simple forms similar to the equations (1) and (3) as for nonparabolic and parabolic respectively and given as,

$$E^h = \frac{\hbar^2 k_z^2}{2m^* a_0^h} + \sqrt{\left(\frac{\gamma Be}{\hbar} + c^2\right)} - c... \quad (6)$$

The nonparabolicity factor a_o^h for hyperbolic band structure is,

$$a_o^h = \frac{\hbar^2}{m^*\gamma}\sqrt{\left(\frac{\gamma Be}{\hbar} + c^2\right)}... \quad (7)$$

Figure of merit

The figure of merit Z is expressed as [2-4],

$$Z = S^2\left(\frac{\sigma}{\kappa}\right)... \quad (8)$$

where, S and $\kappa\,(=\kappa_e + \kappa_1)$ are Seebeck coefficient and thermal conductivity respectively. The electronic conductivity (σ) is given by,

$$\sigma = ne\mu \ldots \quad (9)$$

where n is the concentration of carriers per unit volume and μ is the mobility. The mobility of electrons in the EQL [14] can be expressed as,

$$\mu = \frac{2e}{\sqrt{\pi}m^* a_o}\langle\tau\rangle \quad (10)$$

The symbol $\langle\tau\rangle$ in equations (10) indicates the average over the carrier distribution function. For a nondegenerate semiconductor, the mobility relation given by equation (10) in the case of EQL [14] becomes,

$$\mu = \frac{2e}{\sqrt{\pi}m^* a_o}\int_0^\infty x^{1/2}\tau(x)\exp^{(-x)}\,dx... \quad (11)$$

where, $\chi = E_{oz}/k_B T$ with , k_B the Boltzmann's constant and T being the electron temperature in Kelvin.

For a degenerate semiconductor the mobility relation is given as [15],

$$\mu = \frac{2e}{m^* a_0}\frac{\int_0^\infty x^{1/2}\tau(x)f_o(1-f_o)dx}{\int x^{-1/2}f_o dx}... \quad (12)$$

Knowing the mobility, from equations (11) and (12) for nondegenerate and degenerate cases, one can obtain the electrical conductivity (σ) also, using equation (9). τ(x) in equations (11) and (12) is the total momentum relaxation time for nonphonon scattering mechanisms such as ionized impurity (in) and alloy disorder (all) scattering, found to be dominant in alloy semiconductor such as MCT at low temperatures and phonon scattering mechanisms such as acoustic phonon via deformation potential (ac), piezoelectric (pz) scattering mechanism dominant at low temperatures and polar optical phonon (pop) scattering mechanism, dominant at high temperatures. The total momentum relaxation time

due to all the scattering mechanisms is obtained by combining them using Matthiessen's rule [16].

Seebeck coefficient also gives an idea of scattering processes operative and the nature of the band structures. In the presence of a temperature gradient parallel to the applied high magnetic field along z-direction, the Seebeck coefficient is given [17] as,

$$S = \frac{\xi}{\nabla_z T} = -\frac{k_B}{e}\left[-\frac{E_F(B)}{k_B T} + \frac{\langle E\tau\rangle}{\langle\tau\rangle k_B T}\right]... \quad (13)$$

The 1st term in the equation (13) gives the magnetic field dependent Fermi level term and the 2nd term is the scattering term in the form of ratio.

The equation (13) is applicable for both degenerate and nondegenerate cases. The Fermi energy term $(E_F(B))$ and the average scattering term $\langle\tau\rangle$ with proper carriers distributions are taken according to the condition of degeneracy i.e. for nondegenerate and degenerate cases separately.

For a semiconductor, there are two separate contributions to the thermal conduction. The conduction due to the vibration of the atoms about their position of the thermal equilibrium (lattice vibrations for crystals) and that due to the mobile charge carriers electrons or holes.

The electronic thermal conductivity, κ_e [18] can be expressed as,

$$\kappa_e = \sigma L T... \quad (14)$$

The Lorentz ratio $L = \mathscr{L}\left(k_B^2/e^2\right)$, where

$$\mathscr{L} = \frac{\langle\tau\rangle\langle E^2\tau\rangle - \langle E\tau\rangle^2}{k_B^2 T^2 \langle\tau\rangle^2}... \quad (15)$$

The expression $\langle E^2\tau\rangle$ is also calculated in the similar way mentioned earlier.

The Lattice thermal conductivity (κ_l) calculation is based on Callaway's phenomenological theory [19]. In Callaway's formula the lattice thermal conductivity is given as,

$$\kappa_l = \left(\frac{k_B}{\hbar}\right)^3 \frac{k_B}{2\pi^2 \nu} T^3 \int_0^{T_D/T} \frac{x'^4 \tau_l e^{x'}}{\left(e^{x'}-1\right)^2} dx'... \quad (16)$$

where, T_D is the Debye temperature. $x' = \hbar\omega/k_B T$, where ω is the phonon frequency. The phonon relaxation time (τ_l) is determined by the phonon boundary scattering [20] i.e. $\tau_l = L'/\nu$, L' is the shortest dimension of the sample. The phonon once strike the boundary of the sample loses all it coherence. Hence τ_l is defined for the shortest length of the sample (L') along with velocity of sound (ν), ν is taken separately for acoustic sound velocity (u_{ac}) and the piezoelectric sound velocity (u_{pz}).

3. Results and Discussions

The material parameters for MCT are taken from the references [13,21]. For hyperbolic band structure the constants are taken as, $\gamma = 48.3 \times 10^{-20} e^2$ and $c = 0.058e$[12]. The calculations have been done with the carrier concentrations of $1 \times 10^{20} m^{-3}$ for nondegenerate MCT, with different nonphonon scattering mechanisms such as ionized impurity (in) and alloy disorder (all) scattering, and phonon scattering mechanisms such as acoustic phonon (ac) via deformation potential, piezoelectric (pz) and polar optical phonon (pop) scattering mechanisms [8,10,11]. The total scattering mechanism is obtained by using the Matthiessen's rule.

Total thermal conductivity is taken as a sum of the thermal conductivity due to electron and the lattice. For the lattice part of the thermal conductivity the boundary scatterings due to acoustic phonon (AC) and piezoelectric (PZ) phonons are taken. The Debye temperature T_D has been taken as 300K [22].

Incorporating the low and high temperature scattering mechanisms such as ionized impurity (in), alloy disorder (all), acoustic phonon via deformation potential (ac), piezoelectric (pz) and polar optical phonon (pop) scattering mechanisms,

the variations of ZT with temperature at a constant magnetic field 4.0T for nondegenerate MCT, considering parabolic, nonparabolic and hyperbolic band structures are calculated and is shown in Fig. 1. With the same scattering mechanisms as described above for Fig.1, the variation of ZT with magnetic field at a constant temperature 77 K for nondegenerate MCT, with all three types of band structures is also shown in the Fig. 2.

It is observed from Figs. 1-2, that the value of ZT be maximum for parabolic band structure and is followed by the nonparabolic and then hyperbolic band structures. It is expected because ZT is a function of conductivity (σ), Seebeck coefficient (S), temperature (T) and the thermal conductivity (κ). The thermal conductivity (κ) is a combination of thermal conductivity due to electron (κ_e) and due to lattice (κ_1). The lattice thermal conductivity (κ_1), highly dominates the electronic thermal conductivity (κ_e) and hence the total thermal conductivity (κ). is found to be decreasing with temperature. However, the lattice thermal conductivity is independent of the magnetic field, is also not effected by the band structures. S for hyperbolic band structure is found to be maximum and is followed by the nonparabolic and then the parabolic band structures. However, the mobility for the parabolic band structure is found to be maximum and is followed by nonparabolic and then hyperbolic band structures [15]. Hence, the overall effect causes the ZT for parabolic band structure to be maximum.

The variation of ZT with temperature at a constant magnetic field 4T for nondegenerate MCT, considering only hyperbolic band structure with the same low and high temperature scattering mechanisms used in the Fig. 1 and polar optical phonon (pop) scattering mechanism, a high temperature scattering mechanism separately is shown in Fig. 3. Whereas the Fig. 4 shows the variation of ZT with magnetic field at a constant temperature 77K for nondegenerate MCT, considering only hyperbolic band structure with the same combination of scattering mechanisms used in the Fig. 3.

Both Figs. 3 and 4 shows that the magnitude of ZT for the curve due to polar optical phonon (pop) scattering mechanism be higher compared to the curve given by the total scattering mechanisms. It shows that the polar optical phonon (pop) scattering mechanism highly dominates over the other scattering mechanisms. It is also observed that the difference in the values of ZT between two curves be significant at high temperatures and low magnetic fields.

The variation of ZT with temperature at a constant magnetic field 4T for nondegenerate MCT, considering only hyperbolic band structure for low temperature nonphonon and phonon scattering mechanisms separately is shown in the Fig. 5. Whereas, Fig. 6 shows the variation of ZT with magnetic field at a constant temperature 77K for nondegenerate MCT, considering only hyperbolic band structure with the same combination of low temperature scattering mechanisms as that used in the Fig. 5.

From both Fig. 5 and 6 it is observed that the ZT due to phonon scattering mechanisms highly dominates the ZT due to nonphonon scattering mechanisms. In addition it is also found the difference in the value of ZT be more prominent at high temperatures and low magnetic fields. The use of novel MCT superlattices was also done for the purpose [24-26] i.e. superlattice of $Hg_{0.2}Cd_{0.8}Te/Hg_{0.8}Cd_{0.2}Te$ [26]. According to the author, the reason for the low value of ZT in MCT bulk is due to its very low effective mass and a single conduction band [26]. Both the properties of MCT are considered by authors in the present calculation also.

Hagelstein and Kucherov [27] examined the thermally induced open circuit voltage for $Hg_{0.86}Cd_{0.14}Te$ thermal diode (500 μm) using InGe eleuteric to make contact on both the emitters and collector sides. However, the figure of merit have been measured in $Hg_{0.86}Cd_{0.14}Te$ [27] is without the magnetic field. We have

compared our results for the sake of qualitative understanding. The results show that the value of Z increases with temperature reaches maximum around about 90K and then decreases. A similar variation of dependences of Z for degenerate $Hg_{0.8}Cd_{0.2}Te$ is also found in our calculation.

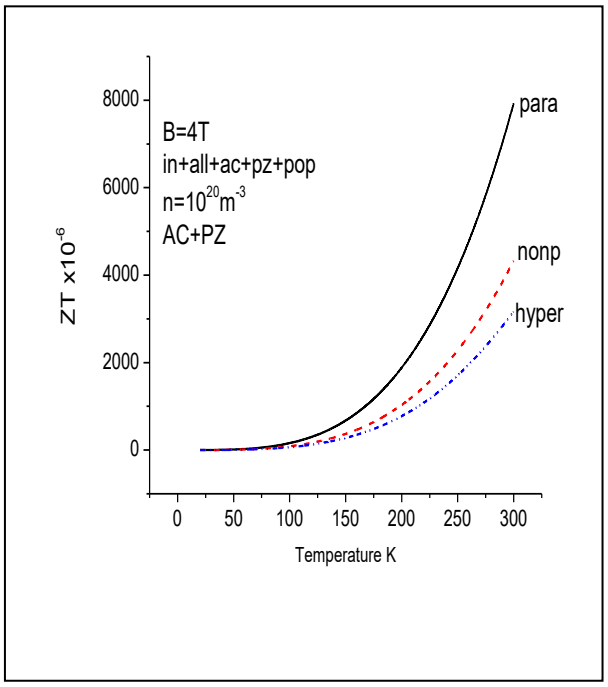

Fig. 1: Variation of ZT with temperature at a constant magnetic field 4T for nondegenerate n-$Hg_{0.8}Cd_{0.2}Te$, considering parabolic (para), nonparabolic (nonp) and hyperbolic (hyper) band structures with various scattering mechanisms such as ionized impurity (in), alloy disorder (all), acoustic phonon via deformation potential (ac), piezoelectric (pz) and polar optical phonon (pop) scattering mechanisms. Boundary scatterings due to acoustic phonon (AC) and piezoelectric (PZ) are included for lattice thermal conductivity.

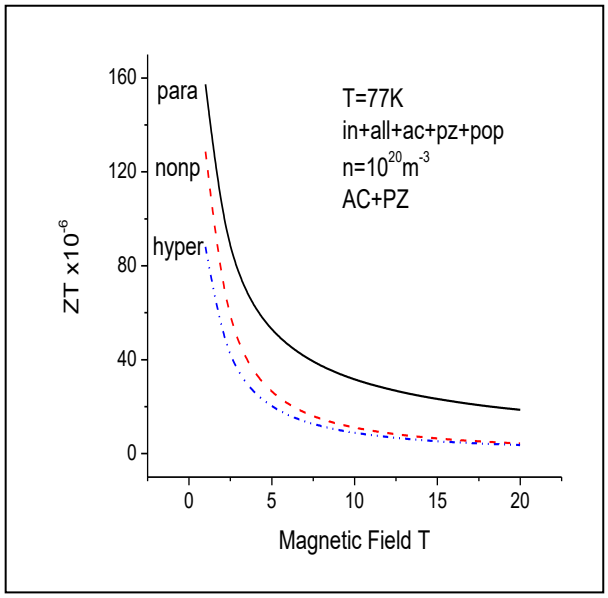

Fig. 2: Variation of ZT with magnetic field at a constant temperature 77K for nondegenerate n-Hg0.8Cd0.2Te, considering all the band structures and with the same scattering mechanisms used in the Fig. 1.

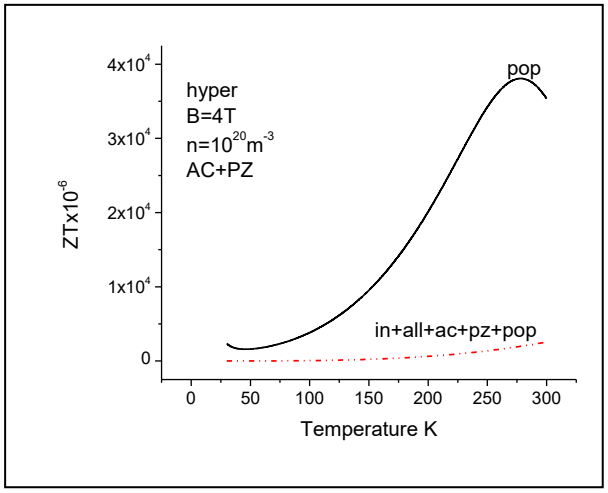

Fig. 3: Variation of ZT with temperature at a constant magnetic field 4T for nondegenerate n-$Hg_{0.8}Cd_{0.2}Te$, considering only hyperbolic (hyper) band structure with the same scattering mechanisms used in the Fig. 1 and only polar optical phonon (pop) scattering mechanism separately.

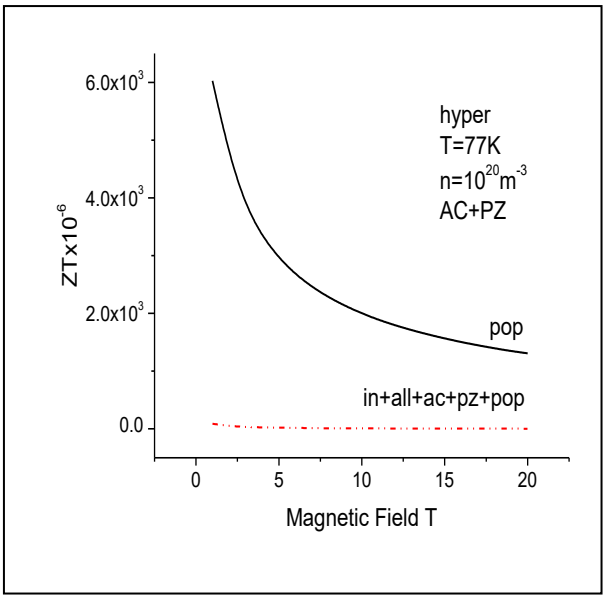

Fig. 4: Variation of ZT with magnetic field at a constant temperature 77K for nondegenerate n-$Hg_{0.8}Cd_{0.2}Te$, considering only hyperbolic (hyper) band structure with the same scattering mechanisms used in the Fig. 1 and only polar optical phonon (pop) scattering mechanism separately.

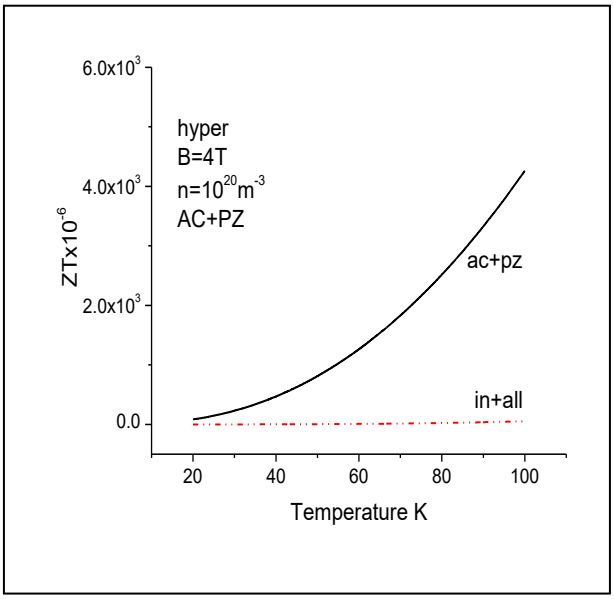

Fig. 5: Variation of ZT with temperature at a constant magnetic field 4T for nondegenerate n-$Hg_{0.8}Cd_{0.2}Te$, considering only hyperbolic (hyper) band structure with low temperature phonon (ac+pz) and nonphonon (in+all) scattering mechanisms.

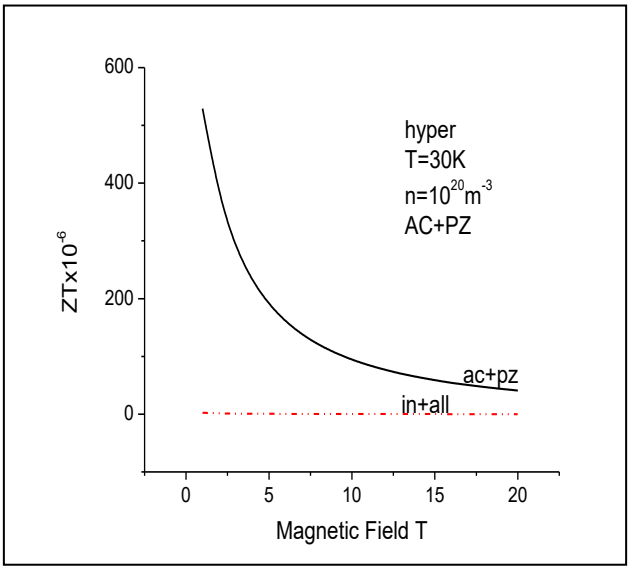

Fig. 6: Variation of ZT with magnetic field at a constant temperature 77K for nondegenerate n-Hg0.8Cd0.2Te with low temperature phonon (ac+pz) and nonphonon (in+all) scattering mechanisms.

4. Conclusions

The magnitude and variation of ZT is found to be maximum for MCT with parabolic band structure is followed by nonparabolic and hyperbolic band structures for all ranges of variation of temperature as well as magnetic field.

ZT due to polar optical phonon scattering mechanism dominates the total ZT given by all the low and high temperature scattering mechanisms for the overall ranges of temperatures as well as for all magnetic fields. But the higher difference in the value of ZT is observed at high temperatures and low magnetic fields for nondegenerate MCT.

In the low temperatures, ZT due to phonon scattering mechanisms dominates the values of ZT due to nonphonon scattering mechanisms for all temperatures and magnetic fields.

Acknowledgements

CKS wishes to thank UGC, Government of India

and Nanotechnology and Science Centre JU, Kolkata for financial support. S. Shrestha sincerely thanks TWAS for providing her TWOWS fellowship to carry out the research work.

References

[1] L. D. Landau, Diamagnetism of metals, S. Physik 64 (1930) 629.

[2] T. C. Harmon and J. M. Honig, Theory of Galvano-Thermomagnetic Energy Conversion Devices. II. Refrigerators and Heat Pumps, J. Appl. Phys. 33 (1962) 3178. https://doi.org/10.1063/1.349091

[3] P. Ed. Egli, Thermoelectricity, Wiley New York, 1961. pubs.acs.org/doi/pdf/10.1021/ed038p534.2

[4] D. M. Rowe and C. M. Bhandari, Modern Thermoelectrics (Reston, Reston VA), 1983.

[5] J. O. Sofo, G. D. Mahan and J. Baars, Transport coefficients and thermoelectric figure of merit of n-$Hg_{1-x}Cd_xTe$, J. Appl. Phys. 76 (4) (1994) 2249. https://doi.org/10.1063/1.357643

[6] A. Shakouri and Chris LaBounty, Pro. of Int. Conf. on Thermoelec. Baltimore, Sept.1999.

[7] H. J. Goldsmid, Electronic Refrigeration, [Pion, London], 1986.

[8] U. P. Phadke and S. Sharma, Longitudinal magnetoresistance in the Extreme Quantum Limit in nonparabolic semiconductors, J. Phys. Chem. Sol. 36 (1975) 1-6. https://doi.org/10.1016/0022-3697(75)90123-7

[9] An. Ban. Chen, CPA band calculation for (Hg, Cd) Te, J. Vac. Sci. Technol. 21 (1982) 138.

[10] V. K. Arora and M. Jaafrian, Effect of nonparabolicity on Ohmic magnetoresistance in semiconductors, Phys. Rev. B 13 (1976) 4457. https://journals.aps.org/prb/abstract/10.1103/PhysRevB.13.4457

[11] V. K. Arora and H. N. Spector, Quantum-limit magnetoresistance for impurity scattering, Phys. Stat. Sol. (b) 94 (1979) 323. https://doi.org/10.1002/pssb.2220940138

[12] S. Krishnamurthy and A. Sher, Temperature dependence of band gaps in HgCdTe and other semiconductors, J. Elec. Mater. 24 (1995) 1121. https://link.springer.com/article/10.1007/BF02653063

[13] S. Krishnamurthy and A. Sher, Electron mobility in Hg0.78Cd0.22Te alloy, J. Appl. Phys. 75 (12) (1994) 7904. https://doi.org/10.1063/1.356576

[14] D. Chattopadhya and B. R. Nag, Warm electrons in polar semiconductors, J. Phys. C 9 (1975) 3095. https://iopscience.iop.org/article/10.1088/0022-3719/9/16/015/meta

[15] P. Banerje, Ph. D. Thesis, Jadavpur Univerity, Kolkata, 1995.

[16] A. Mathiessen, Ann. Phys. Chem. 7 (1964) 761, 892.

[17] B. R. Nag, Electron Transport in Compound Semiconductors Vol. II, edited by H.J. Queisser (springer Berlin), 1980. 10.1007/978-3-642-81416-7

[18] R. A. Smith, Semiconductors, Academic Publishers, IInd edition, 1989.

[19] J. Callaway, Model for Lattice Thermal Conductivity at Low Temperatures, Phys. Rev. 113 (4) (1959) 1046. https://doi.org/10.1103/PhysRev.113.1046

[20] S. M. Puri and T. H. Geballe, Semiconductors and Semimetals 1 ed. by R.K. Willardson and A.C. Beer (Academic, New York) 254, 1966.

[21] R. Dornhaus and G. Nimtz, The properties and applications of the $Hg_{1-x}Cd_xTe$ alloy system, Springer Tracts in Mod. Phys. 98 (1983) 119. https://link.springer.com/chapter/10.1007/BFb0044921

[22] J. P. Stadler and G. Nimtz, Heat capacity of a condensed electron system in the dilute metal n-$Hg_{0.8}Cd_{0.2}Te$, Phys. Rev. Lett. 56 (4) (1986) 382.

[23] D. Vashaee and A. Shakouri, Phys. Rev. Lett. 92 (2004) 106103. https://doi.org/10.1103

[24] D. Vashaee and A. Shakouri, Electronic and thermoelectric transport in semiconductor and metallic superlattices, J. Appl. Phys. 95 (2004) 1233. https://doi.org/10.1063/1.1635992

[25] R. J. Radtke, H. Ehrenreich, and C. H. Grein, Multilayer thermoelectric refrigeration in $Hg_{1-x}Cd_xTe$ superlattices, J. Appl. Phys. 86 (1999) 3195. https://doi.org/10.1063/1.371188

[26] D. Vashaeea_ and A. Shakouri, HgCdTe superlattices for solid-state cryogenic refrigeration, Appl. Phy. Lett. 88 (2006) 132110. https://doi.org/10.1063/1.2191094

[27] P. L. Hagelstein and Y. Kucherov, Enhanced figure of merit in thermal to electrical energy conversion using diode structures, Appl. Phys. Lett. 81 (3) (2002) 559. https://doi.org/10.1063/1.1493224